Calculation of efficiency of work of converters of energy of solar heat and electric stations

Nikolay Moskalenko, *Maryana* Khamidullina and *Azat* Akhmetshin*

Kazan State Power Engineering University, 420066 Kazan, str. Krasnoselskaya 51, Russia

Abstract. The modeling of complex radiation heat exchange in the system "Sun-atmosphere-solar thermal and electric stations" is considered. The structural scheme of solar radiation inflows to the heat-absorbing surface of solar thermal and electrical stations is discussed. Calculations of spectral intensities and the flux of solar radiation, taking into account the selectivity of molecular absorption of radiation by the ingredients of the gas phase of the atmosphere, scattering and absorption of radiation by atmospheric aerosol and clouds, taking into account the statistics of their distribution depending on the location of the station and the time of year. Modeling of anthropogenic impacts on the operation of solar thermal and electrical stations in connection with the capture of anthropogenic emissions of sols by clouds is performed. An assessment of the impact of economic activity on the work of promising solar thermal and electrical stations. The developed methods for calculating the spectral intensities and fluxes of short-wave and long-wave radiation on the underlying surface make it possible to calculate the efficiency of the functioning of solar hot water supply systems for any location and structural solution.

1 Introduction

Solar energy is one of the areas of alternative energy, which develops the scientific foundations, methods and technical means of using solar radiation energy on Earth and in space to convert it into thermal, mechanical and electrical energy, as well as into other types of energy, and determines the areas and scales of effective use of solar energy [1-3].

Solar power stations today generate about 0.04% of the total energy, and at the moment they cannot yet compete with thermal power plants, nuclear power plants, hydroelectric power plants. The idea of using the energy of the Sun is one of the main ones for solving the problem of energy saving in the future. Solar power plants work in heating and cooling systems of buildings, in technological processes that take place at any temperature. There are many different technological schemes for converting SR into electrical energy on the basis of thermal cycles, thermoelectric and thermionic processes widely known in technology [1,4,5].

The main modern types of solar power plants:

- solar thermal power plants;
- solar photovoltaic stations;
- solar ponds, etc.

Solar photovoltaic plants use the method of direct transformation of solar energy into electrical energy using photovoltaic converters, which are most widely used in the world. They are also called photovoltaic modules, solar panels, solar modules.

Solar radiation incident on the receiving system includes direct illumination of radiation weakened by the atmosphere, solar radiation scattered by atmospheric aerosol, scattered solar radiation by clouds, which undergo significant spatio-temporal variations with the time of year and day due to a change in the place of observation and overlapping of the sky with clouds of the lower, middle and the upper tiers. In this work, we use the modeling of the structural and optical characteristics of the atmosphere, developed in [2-4] with the use of statistics [5,6].

The developed methods for calculating the spectral intensities and fluxes of short-wave and long-wave radiation on the underlying surface [2–6] make it possible to calculate the efficiency of solar hot water supply units for any location and design solution. The most efficient installations of solar hot water supply with a system of automated orientation of the heat-receiving surface to the solar disk [1]. In this case, the heat absorption of solar radiation in the solar hot water installation will be the maximum possible. The orientation of the heat-sensing surface should be carried out both in the zenith and azimuthal angles, taking into account the temporal variations in the position of the Sun in the sky.

Solar fluxes are calculated for any localization of the location of the solar hot water installation [7]. In the case of a horizontal or inclined arrangement of the heat-receiving surface of the solar hot water supply installation, it is necessary to introduce the effective area of the heat-absorbing surface. In the calculations, it is necessary to take into account the selectivity of absorption spectra of solar radiation by atmospheric gases of direct and scattered solar radiation, diffuse

* Corresponding author: dr.akhmetshin@ieee.org

diffuse reflected solar radiation from the underlying surface into the rear hemisphere, thermal counter-radiation of the atmosphere incident on the heat-absorbing surface, heat losses due to convective heat exchange and external radiation cooling.

If the heat-receiving surface is "black", and there is no heat transfer to the rear hemisphere, then the maximum possible temperature of the coolant Tmax can be determined from the radiation balance between the incoming flow of solar radiation and the intrinsic thermal radiation of the heat-receiving surface. For example, at an atmospheric temperature Ta = 300 K, and the position of the Sun with a zenith angle $\theta_0 = 0$ ° Tmax≈420 K. The actual temperature of the coolant in the solar collector will always be below Tmax and will depend on the zenith angle of the Sun θ_0, the angle of inclination of the collector plane to the horizon θ_0^* and azimuth angle φ^*, collector area, meteorological state of the atmosphere, hot water supply D capacity, solar collector design.

2 Method for calculating the efficiency of energy converters of solar thermal power plants

Let us further consider a method for calculating the efficiency of converters of solar thermal power plants, taking into account the statistical characteristics of the meteorological state of the atmosphere, which is characterized by high spatio-temporal variability, one of the factors of which is anthropogenic disturbances of the atmosphere and anthropogenic effects on the protective coatings of the converter. The total radiation flux reaching the heat-sensing surface of the transducer is determined by the relation:

$$F^*(t)=\sum_i f\left[\bar{F}_i\left(s,\theta_0^*,\varphi^*,t\right)P_i\left(\theta_0^*,\varphi^*\right)+\bar{F}_{iT}^*(t)+\bar{F}_{iT}(t)P_{iT}+\right]+\int_\lambda\sum_i \bar{F}_{i\lambda}\left(s,\theta_0^*,\varphi^*,t\right)\delta_\lambda^*\delta_\lambda d\lambda, \quad (1)$$

where $\bar{F}_i$ is the average monthly or daily solar radiation flux incident on the glass (film) coating of the solar converter, where f_i is the probability of a situation manifestation i, i is the situation number (clearly, one-tier cloudiness of the lower, middle and upper tiers, two-tier overlap of the lower and middle tiers, two-tier overlap of the lower and upper tiers, two-tier overlap of the middle and upper tiers, three-tier overlap of the sky with clouds of the lower, middle and upper tiers; in this case, the condition $\sum_i f_i = 1$; s is satisfied the area of the heat-sensing surface of the thermal converter; t is time (day, month); δ_λ is spectral albedo of the underlying surface; δ_λ^* is spectral albedo of the atmosphere for diffuse reflected radiation; $\bar{F}_{iT}^*(t)$ is intrinsic thermal radiation of the protective coating, which heats up due to absorption of solar radiation; $\bar{F}_{iT}(t)$ is the flux of thermal counter-radiation of the atmosphere; $P_{iT}(t), P_i^*(t)$ is transparency of the protective coating for thermal radiation and solar radiation for i situation. The values $P_{iT}(t), P_i^*(t)$ are determined by both reflection and absorption of radiation by the protective coating. The values of $P_{iT}(t)$ and $P_i^*(t)$ can also change due to anthropogenic impacts. The radiation flux received by the heat-sensing surface is determined by its emissivity $\bar{\xi}$, so that:

$$F_n^*(t)=F^*(t)\bar{\xi}. \quad (2)$$

By mechanical and technological processing of the heat-absorbing surface it is possible to achieve the values $\bar{\xi}=0,96\div0,98$. It is desirable to cover the back side of the solar collector with a reflective coating to reduce heat losses and to use thermal insulation to reduce external cooling. If we introduce the external cooling coefficient q_{ec}, then the useful perception $F_n^*(t)$ is determined by the ratio:

$$F_n^*(t)=F^*(t)\bar{\xi}q_{\text{ec}}(t). \quad (3)$$

Radiation fluxes $\bar{F}_i\left(s,\theta^*,\varphi^*,t\right)$ are calculated by integrating the spectral intensities of direct illumination of the solar radiation surface and scattered radiation over the wavelength spectrum and solid angle within the hemisphere according to the relationships considered in [2, 3, 7]. Algorithms for calculating the heat fluxes of radiation $\bar{F}_{iT}$ in the Earth atmosphere system are considered in [4]. Note that in the case of overlap of the sky by clouds, the values $\bar{F}_i\left(s,\theta^*,\varphi^*,t\right)$ are determined only by scattered radiation. In all cases, the absorption of radiation by the atmosphere is calculated taking into account the sharp selection of absorption spectra by the gas phase of the atmosphere by the two-parameter method of equivalent mass [4, 7] or by the method of direct numerical simulation of the fine structure of molecular absorption spectra [8-10].

The temperature of the coolant at the outlet of the solar collector is determined from the radiation balance equation:

$$C_p D\Delta T=F^*(t)\bar{\xi}q_{\text{ce}}, \quad (4)$$

where $\Delta T = T - T_{\text{oh}}$, C_p is the heat capacity of water; D is heat and water supply performance; T_{oh} is the temperature of the feed water at the inlet of the solar collector.

To maintain a constant temperature at the outlet of the heat converter, it is necessary to change the water supply performance in proportion to the value $F^*(t)$ during the daylight hours, which is quite problematic to implement. This is the main disadvantage that limits the use of heat and power solar converters.

Let us estimate the influence of anthropogenic influences on the operation of solar hot water supply installations. This effect is manifested due to the increased absorption of solar radiation by industrial emissions of gas ingredients and ash formations into the atmosphere, anthropogenic influence on the distribution of cloudiness over the globe and its temporal variations, an increase in moisture content in the atmosphere as a result of the greenhouse effect of the atmosphere, and an increase in the concentration of tropospheric ozone. It was found that in the vicinity of large cities precipitation is twice as large, which reduces the overlap of the sky by clouds of the lower and middle tiers. The overlap of the sky by clouds decreases as the air mass flows inland. The deposition of soot ash on the protective coating of a solar hot water installation reduces the value $F^*(t)$. Decreasing the cloud cover of the sky increases the value $F^*(t)$. Let us pay attention to the fact that the growth of the optical thickness of the atmosphere due to absorption of radiation by the sol increases in inverse proportion $\cos\theta_0$, and for gaseous components - in inverse proportion $(\cos\theta_0)^m$, where m takes different values for different ingredients in the range $\{0,4;0,8\}$. In this regard, the degree of the influence of the sol on the decrease in the value $F^*(t)$, in comparison with the effect of the gas ingredients, increases with an increase in the zenith angle $\theta_0(t)$ of observation of the Sun. Anthropogenic impacts on the influx of solar radiation are manifested through its absorption by hydrocarbons, nitrogen oxides, ozone, industrial ash, sulfur dioxide by anthropogenically disturbed clouds.

A decrease in the efficiency of a solar hot water supply installation is determined by the reflection of solar radiation from the protective coating and heat losses for external cooling, the difference in emissivity from unity $(\bar{\xi} \prec 1)$, absorption of solar radiation by the protective coating. The quantity:

$$P_i\left(\theta_0^*, \varphi^*\right) = \bar{\delta}_i\left(\theta_0^*, \varphi_0^*\right) \cdot \bar{\tau}_i\left(\theta_0^*, \varphi_0^*\right), \qquad (5)$$

were

$$\bar{\delta}_i\left(\theta_0^*, \varphi_0^*\right) = \left(\bar{n}^2 - 1\right)\left(\bar{n}^2 + 1\right), \qquad (6)$$

$$\bar{\tau}_i = \bar{k}\exp\left(-2\bar{k}d_i\right), \qquad (7)$$

$\bar{n}$ is the real part of the refractive index; $\bar{k}$ is absorption coefficient of the protective coating material; d_i is the effective sheeting thickness for the situation i.

In the case of a two-layer protective coating:

$$P_i\left(\theta_0^*, \varphi^*\right) = \bar{\delta}_i^2\left(\theta_0^*, \varphi^*\right) \cdot \bar{\tau}_i^2\left(\theta_0^*, \varphi_0^*\right). \qquad (8)$$

Table 1 shows the reflection coefficients δ for glass, obtained taking into account multiple re-reflection depending on the zenith angle of incidence of solar radiation θº on the surface of the solar hot water supply.

Table 1. Dependence of the quantities δ and δ^2 on the zenith angle of the Sun θº

Zenith angle θº	δ	δ^2
0º	0,925	0,85
30º	0,92	0,84
60º	0,85	0,72
70º	0,78	0,53

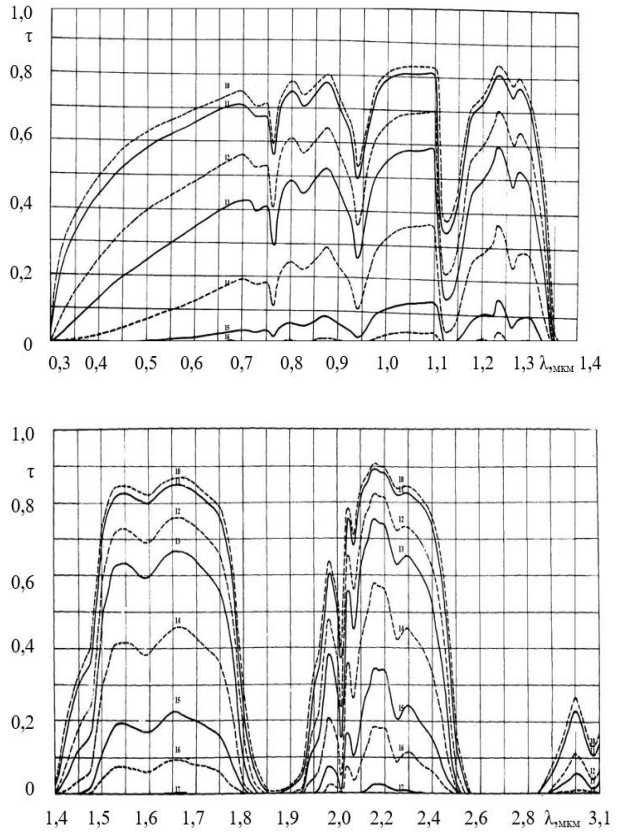

Fig. 1. Spectral transparency of the atmosphere in the spectral range of 0.3-3.1 μm at zenith viewing angles θ (z_1): 10–0^0, 11–30^0, 12–60^0, 13–70^0, 14–80^0, 15–85^0, 16–87^0, 17–89^0, 18–90^0, 19–$90^0$20 '.
a) spectral region 0.3–1.04 μm; b) spectral region 1.4-3.1 μm

In the case of a solar power stations, a solar thermal stations, a system of mirrors serves as a receiving surface

for solar radiation, focusing the radiation on the surface of the pipe system of the steam generator. The steam capacity *D* of the steam generator is calculated from the energy balance between the useful solar radiation flux coming to the mirror system and the heat energy of the steam (enthalpy of the heat carrier + its phase transition energy).

When modeling the optical characteristics of atmospheric, anthropogenic aerosols and clouds, an electronic database of optical characteristics was used, prepared using the calculated data of polydisperse ensembles of particles of various chemical compositions, developed in the interests of global modeling of radiation heat transfer [10] and in environments disturbed by strong natural and anthropogenic impacts [11-13].

3 Influence of anthropogenic emissions into the atmosphere on the efficiency of functioning of solar photovoltaic stations

In the case of using photovoltaic modules as radiation receivers, the perceived flux of solar radiation is converted into electrical energy of solar cells and is determined by the ratio

$$W = \int_{\Delta\lambda} F_{\lambda b}\downarrow \cdot \delta_{\lambda a} \cdot \eta_{\lambda} d\lambda, \qquad (9)$$

where $F_{\lambda b}\downarrow$ is the spectral flux of solar radiation at the outer boundary of the atmosphere; η_{λ} is spectral dependence of the conversion coefficient of solar radiation into electrical energy; $\Delta\lambda$ is spectral range of photocell sensitivity.

In the case of a cloudless atmosphere, for calculating solar radiation fluxes, it is advisable to use the method of expanding the solution in terms of the scattering multiplicity, which makes it possible to take into account the absorption of radiation in the atmosphere scattering radiation using the analytical spectral transmission functions [7]. For a cloudy atmosphere, the most reliable application of the multi-stream approximation method in calculating the downward radiation flux $F\downarrow$. Direct illumination of solar radiation $F_{\text{P}}^{\downarrow}$ from receiving sites is taken into account according to the transparency spectra of the atmosphere [10]:

$$F_{\text{P}}^{\downarrow} = \int_{\Delta\lambda} F_{\lambda S}(\theta)\downarrow \cdot \tau_{\lambda}(\theta) d\lambda, \qquad (10)$$

where $F_{\lambda S}\downarrow$ is the spectral irradiation of the outer boundary of the atmosphere by the Sun; θ - zenith angle. For example, Tables 2 and 3 show the dependences of the spectral albedos $\delta_{\lambda a}$ in the spectral range of 0.3–0.8 μm for different zenith angles of the Sun θ of a cloudless atmosphere. Daily variations of θ from time of day are calculated using an online calculator [7] for any place in the world.

Table 2. Spectral albedo of a cloudless background atmosphere when observed from the underlying surface (θ is the zenith angle of the Sun, λ is the wavelength)

θ, °	λ, μm					
	0,300	0,400	0,500	0,550	0,600	0,800
0,0	0,01758	0,1722	0,0864	0,0624	0,0489	0,025
5,0	0,01708	0,1845	0,0986	0,0725	0,0585	0,031
10,0	0,01658	0,1967	0,1109	0,0825	0,0680	0,037
15,0	0,01608	0,2006	0,1137	0,0926	0,0775	0,043
30,0	0,01457	0,2193	0,1263	0,1036	0,0870	0,048
45,0	0,01197	0,2555	0,1506	0,1240	0,1045	0,059
60,0	0,00828	0,3241	0,1994	0,1652	0,1402	0,081
75,0	0,00515	0,4632	0,3161	0,2652	0,2293	0,144
80,0	0,00511	0,5360	0,3934	0,3325	0,2919	0,197
85,0	0,00506	0,6127	0,5015	0,4253	0,3844	0,314

Table 3. Spectral albedo of a cloudless atmosphere with urban haze when observing counter-radiation from the underlying surface (θ is the zenith angle of the Sun, λ is the wavelength)

θ, °	λ, μm							
	0,300	0,347	0,400	0,500	0,550	0,600	0,694	0,800
0,0	0,0175	0,1250	0,1111	0,0624	0,0519	0,0411	0,0301	0,0216
5,0	0,0169	0,1321	0,1245	0,0692	0,0611	0,0584	0,0369	0,0274
10,0	0,0161	0,1392	0,1353	0,0784	0,0713	0,0599	0,0428	0,0314
15,0	0,0159	0,1462	0,1405	0,0795	0,0801	0,0694	0,0459	0,0336
30,0	0,0141	0,1519	0,1654	0,0899	0,0824	0,0782	0,0541	0,0386
45,0	0,0111	0,1532	0,1896	0,1154	0,1114	0,0899	0,0614	0,0486
60,0	0,0081	0,2163	0,2511	0,1610	0,1433	0,1198	0,0812	0,0649
75,0	0,0050	0,2281	0,3214	0,2594	0,2141	0,1508	0,1622	0,0999
80,0	0,0049	0,3003	0,4192	0,3114	0,2645	0,2251	0,1914	0,1391
85,0	0,0048	0,3167	0,4853	0,4153	0,3664	0,3116	0,2863	0,2342

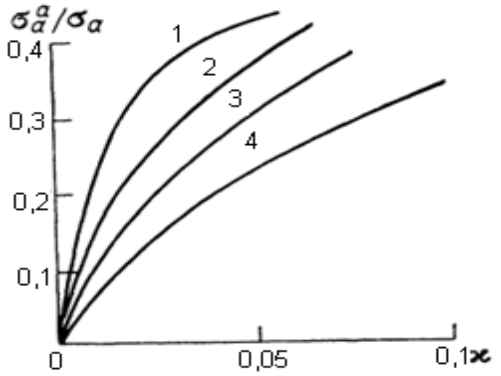

Fig. 2. Dependence of the ratio of spectral coefficients σ_a^a/σ_a on the imaginary part of the complex refractive index for different wavelengths λ, μm:
1 - 0.3; 2 - 0.69; 3 - 1.06; 4 - 1.7

In fig. 2 shows the dependence of the ratio of the spectral coefficients σ_a^a/σ_a of the absorption cross sections σ_a^a to the radiation attenuation cross section σ_a on the imaginary part of the complex refractive index χ for polydisperse urban aerosol at different wavelengths λ, which characterize the strong dependence of the optical characteristics of atmospheric aerosol on anthropogenic emissions of soot ash. A characteristic feature of soot ash is the fact that particles of soot ash practically do not scatter radiation into the rear hemisphere [11-13].

Soot sol has a significant effect on the optical characteristics of cloud particles due to the capture of a finely dispersed fraction of soot sol by cloud particles. The flow of particles diffusing into the cloud is determined by the relationship [14-15].

$$F_p = \int_R \int_r 4\pi R D(r) \frac{\partial N(r)}{\partial r} dr \frac{\partial N(R)_0 dR}{\partial R}, \qquad (11)$$

where $D(r)$ is the diffusion coefficient of particles (varies in the range $10^{-5} \div 10^{-6}$ cm^2/sec for particles larger than 0.1 μm); $\frac{\partial N(r)}{\partial r}$ is distribution of the number of aerosol particles in a volume of 1 cm^3; $\frac{\partial N(R)}{\partial R}$ is distribution of the number of cloud particles in a volume of 1 cm^3; r, R are the radii of aerosol and cloudiness particles. For the number density of cloud $N_0 = \int \frac{\partial N(R)}{\partial R} dR = 10^3 \, см^{-3}$ particles and the number density of aerosol $N_a = \int \frac{\partial N(r)}{\partial r} dr = 10^5 \, см^{-3}$ particles, ≈10% of the smoke particles will be captured within one hour, and ≈30% of the smoke within the cloud cover will be captured by the cloud during the cloud lifetime of $\tau_0 =$ 3 hours.

Due to an increase in the effective absorption cross section of a cloud particle, the latter evaporate, forming giant particles with a radius of $r > 0{,}5$ μm, which are deposited as a result of sedimentation on the underlying surface. Smaller particles can serve as condensation nuclei to form a new cloud. This process of purifying the atmosphere from smoke and dust ash is more efficient than conventional coagulation. Its effectiveness can be enhanced by the electrical properties of the charged particles.

For homogeneous coagulation of particles, the temporal growth of a particle is described by a simple model:

$$r/r_0 = \left[1 + \frac{1}{2} K n_0 \frac{\ln(1+\alpha t)}{\alpha}\right]^{1/3}, \qquad (12)$$

where K is the coefficient of Brownian coagulation; n_0 is the number of particles per unit volume;

α^{-1} is the time during which the particle size will double.

For heterogeneous multicomponent coagulation of particles, the distribution of the number of particles $f[r(t)]$ is determined by the relation [15]:

$$\frac{f[r(t)]}{f_0(r)} = \sum_i \left[1 + \frac{1}{2} k_i n_{0i} \ln\left\{\frac{1+\alpha_i t}{\alpha_i}\right\}\right]^{1/3} + \sum_{i \neq k} \left[1 + \frac{1}{2} k_{ik} (n_{oi} \cdot n_{ok})^{1/2} \cdot \ln\left\{\frac{1+\alpha_{ik} t}{\alpha_{ik}}\right\}\right]^{1/3} \qquad (13)$$

where $f[r(t)]$ is the time dependence of the particle size distribution; i - fraction number; ki is the Brownian coagulation coefficient for component i; $k_{i,k}$ is coefficient of Brownian interaction of particles of different fractions i, k.

When performing calculations, it is possible to use an iterative procedure in calculations in time Δt. The dependence of albedo δ on the mass concentration of soot is considered in [15]. The coagulation of aerosol particles is strongly influenced by the electrical properties of the particles.

The relations between the efficiency of the solar photovoltaic stations functioning in the conditions of an anthropogenically undisturbed atmosphere and atmosphere, taking into account the impact of urban haze, are determined by

$$\frac{\eta}{\eta_0} = \frac{f_1\left(\int_\lambda F_\lambda(\theta) \cdot \delta_{b\lambda}(\theta) \cdot k_\lambda d\lambda + \int_\lambda F_\lambda(\theta) \cdot \tau_{b\lambda}(\theta) \cdot k_\lambda d\lambda\right) + f_1\left(\int_\lambda F_\lambda(\theta) \cdot \delta_\lambda(\theta) \cdot k_\lambda d\lambda + \int_\lambda F_\lambda(\theta) \cdot \tau_\lambda(\theta) \cdot k_\lambda d\lambda\right) + f_2\left(\int_\lambda F_\lambda(\theta) \cdot \delta_{0b\lambda}(\theta) \cdot k_\lambda d\lambda\right)}{+ f_2\left(\int_\lambda F_\lambda(\theta) \cdot \delta_{0\lambda}(\theta) \cdot k_\lambda d\lambda\right)}, \qquad (14)$$

where k_λ is the spectral dependence of the conversion coefficient of solar radiation; f_1 is the probability of a cloudless state of the atmosphere; f_2 is the probability of overlapping the sky with clouds, $f_1 + f_2 = 1$.

In fig. 3–4 show, for example, the calculated efficiencies $\eta(\theta)$ and ratios of the functioning efficiency $\frac{\eta(\theta)}{\eta_0(\theta)}$ in a cloudless atmosphere and the atmosphere, taking into account urban haze, depending on the zenith angle of the Sun, of silicon photovoltaic modules with a thin film of chalcogenides (cadmium coating *CdTe*/*CIS*/*CIGS* with a film thickness of 1.25 μm) for latitude 45^0 for the month of June at the optical thickness of clouds $\tau_0 = 10.$ The spectral conversion coefficient of solar radiation k_λ is taken from the literature [16, 17].

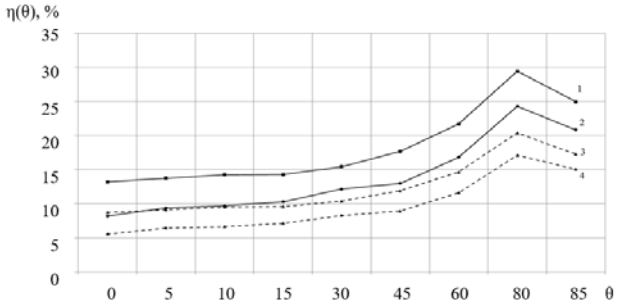

Fig. 3. The efficiency of functioning in an anthropogenically cloudless atmosphere and atmosphere, taking into account urban haze for silicon photovoltaic modules (1, 2) and photovoltaic modules with a thin film of chalcogenides (3, 4)

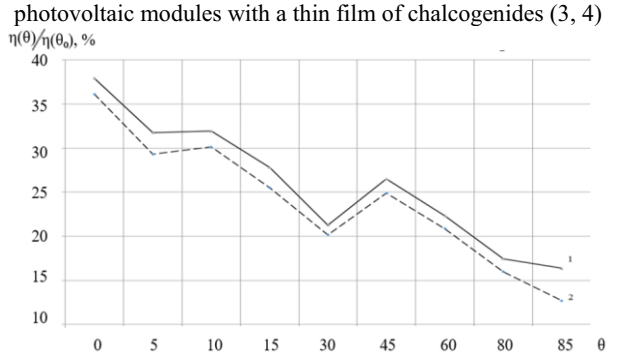

Fig. 4. Ratios of the efficiency of functioning in an anthropogenically undisturbed atmosphere and atmosphere taking into account the urban haze for silicon photovoltaic modules (1) and photovoltaic modules with a thin film of chalcogenides (2)

Comparison of spectral irradiation of solar radiation for the background model of the atmosphere and the atmosphere, disturbed by anthropogenic emissions, shows that anthropogenic impacts on the atmosphere under urban haze conditions underestimate the solar radiation flux on the heat-absorbing surface by an average of 24-30%, reducing the efficiency of the solar thermal power plants. The effect of cloud pollution with industrial soot aerosol on the irradiance of the solar radiation receiver of a solar power plant has a more significant effect. For example, with the thickness of the pure cloud cover $\tau_0 = 5$, the scattered solar radiation reaching the heat-receiving surface is 45% of the solar radiation flux *Wp* at the outer boundary of the atmosphere, while the decrease in the probability the survival of the quantum to the value $\omega_0 = 0.98$, due to the capture of the soot ash cloud by the particles, leads to a decrease in the irradiation of solar radiation on the heat-sensing surface to a value of 27% of *Wp*. The decrease in the efficiency of the solar thermal power plants functioning will be 40%. Due to the significant influence of anthropogenic disturbances on the efficiency of the solar power plant, they must be located outside the city limits. With an increase in the optical thickness of the cloud, the solar radiation flux to the heat-receiving surface decreases and, consequently, the efficiency of the solar power plant functioning decreases.

4 Conclusions

In conclusion, let us dwell on the main results obtained in this work.

Numerical simulation of radiation heat transfer is advisable to use to substantiate the methods of operational modeling and identify errors in their application, depending on the spectral characteristics of the radiation propagation medium. The developed database on the spectral optical characteristics of the ingredients of the gaseous phase of the atmosphere, atmospheric aerosol and multi-level cloud control, and atmospheric anthropogenic emissions. Calculations of solar power plants in a clean atmosphere and an atmosphere disturbed by anthropogenic pollution have been performed. Pollution of the atmosphere with soot ash significantly reduces the efficiency of solar power plants to 40% due to the significant influence of anthropogenic disturbances on the efficiency of solar power plants, it is advisable to replace them outside the city limits. With an increase in the optical thickness of clouds, the flux of solar radiation on the heat-sensing surface also decreases and, therefore, the efficiency of the functioning of solar power plants decreases.

References

1.Gibilenko C. Alternative energetics without the mystery, Moscow ERsmo, p.308 (2010)
2.Kondratiev K.Ya., Moskalenko N.I. The greenhouse effect of the atmosphere, Moscow, VINITI edition, p. 224 (1984)
3.Kondratiev K.Ya., Moskalenko N.I. Thermal radiation of planets, Leningrad, Hidrometioedition, p. 264 (1977)
4.Kondratiev K.Ya., Moskalenko N.I. Posdnyakov V.D. Atmospheric aerosol, Leningrad, Gidrometioedition, p.224 (1983)
5. Krapivin V.F., Kondratiev K.Ya. Environmental global change: ecoinformatics, St. Peterburg, p.723 (2002)
6. Kondratiev K.Ya., Donchenko V.K. Ecodinamics and geopolitics, St. Peterburg, **1**, p.1032 (1999)
7. Moskalenko N.I., Mirumyants S.O. Atlas of spectral transmittance of the atmosphere on arbitrarily direction, Moscow, VINITI edition, p.494 (1979)
8. Moskalenko N.I., Khamidullina M.S., Safiullina Ya.S. Izv. Vuzov, Problems of Energetics, № 3-4, pp.29-39 (2016)
9. Moskalenko N.I., Safiullina Ya.S., Sadykova M.S. Izv. Vuzov, Problems of Energetics, № 1-2, pp.43-54 (2014)
10. Moskalenko N.I., Dodov I.R., Khamidullina M.S. New technology materials and equipments, KGEU edition, **2**, pp.232-238 (2018)
11. Kondratiev K.Ya., Moskalenko N.I., Saferova T.M. DAN SSSR, **318**, № 3, pp. 580-583 (1991)
12. Moskalenko N.I., Safiullina Ya.S., Khamidullina M.S. Izv. Vuzov, Problems of Energetics, № 7-8, pp.3-13 (2014)
13. Moskalenko N.I., Khamidullina M.S. Izv. Vuzov, Problems of Energetics, № 3-4, pp.26-35 (2014)
14. Moskalenko N.I., Safiullina Ya.S., Khamidullina M.S. Alternative Energetics and Ecology, №3(143), pp.48-59 (2014)
15. Moskalenko N.I., Khamidullina M.S., Safiullina Ya.S. Izv. Vuzov, Problems of Energetics, № 3-4, pp.29-39 (2016)
16. Bakhshiev N.G. Science and life №12, pp. 19-25 (2013)
17. www.mash-xx.info.ru